# ON VIRTUAL BOUND STATES IN CAESIUM AND CERIUM

S.Ramaseshan, T.G.Ramesh and V.Shubha
Materials Science Division
National Aeronautical Laboratory
Bangalore 560017

## Abstract

This article reviews the work done at Bangalore on some problems connected with the pressure-induced electronic phase transition in liquid caesium and the phenomenon of valence instability and related narrow band effects in cerium metal. Among the alkali metals, caesium exhibits striking anomalies in several of the physical properties at high pressures. A theoretical model for the phenomenon of electron collapse in the liquid phase is presented which is based on the concept of 'virtual bound state' or 'Scattering resonance'. The result of the numerical calculations based on this model are given which generally explain all the main features of the anomalous resistivity behaviour of liquid caesium with pressure. In the field of valence flectuating systems, new data on the pressure behaviour of the resistivity and thermo-electric power in a typical Anderson lattice system like $\gamma$-Ce are presented. The new observation of Kondo-like anomalies in $\gamma$-Ce and their resonant enhancement with pressure are shown to favour the 4f virtual bound state model developed for cerium.

*Indian Journal of Pure and Applied Physics* 19, 846, 1981

## Electronic Transition in Liquid Caesium

### 1. Introduction

The high pressure behaviour of caesium has been a subject of numerous investigations. The main interest in this substance is centered round the existence of a double maximum in the fusion curve, first established by Kennedy et al (1962) and a later discovery of an iso-structural phase transition near 42 kbar pressure (Hall et al 1964). Figure 1 shows the phase diagram of caesium given by McWhan and Stevens (1969). At 23 kbar pressure, there is a structural phase transition from b.c.c. to f.c.c. The more interesting aspect of the phase diagram is however the iso-structural electronic phase transition near 42.5 kbar pressure which has been attributed to the so called 6S-5d electron collapse (Sternheimer, 1950).

The existence of a double maximum in the fusion curve has strong implications on the density variation with pressure in the liquid phase. The application of the Clausius-Clapeyron equation $dT/dP = \Delta V/\Delta S$ to the melting process leads to the result that at the maxima, the density of liquid caesium is equal to that of the solid phase lying below the corresponding maxima. The negative slopes following the two maxima in the fusion curve imply that the density of the liquid phase is higher than that of the corresponding solid phase. The increase in density immediately after the first maximum can, in principle, be understood as arising due to an increase in the co-ordination

number in the liquid phase relative to the b.c.c. co-ordination. However, this kind of reasoning fails to account for the density variation in the region following the second maximum, as the solid phase underneath is in the closest packed configuration. This anomalous variation in the density of liquid caesium with pressure ie. the liquid becoming denser than the closest packed solid phase, is perhaps the most interesting feature of this substance. Jayaraman et al (1967), based on their resistivity data on liquid caesium upto 50 kbar, postulated that the electron collapse occurs in the liquid phase over a broad pressure range. Ramesh and Ramaseshan (1972) proposed a virtual bound state model for the electronic transition in liquid caesium and also made numerical calculations of the resistivity as a function of pressure on the basis of the Ziman's theory of liquid metals.

## 2. Two Species Model

We shall briefly go into the so called 'two species' model of liquid caesium. It was Klement (see Rapapport 1968) who first suggested that the phenomenon of electron collapse could occur in the liquid phase at a much lower pressure. The two-species model employed by Ramesh and Ramaseshan (1972), Ramesh (1973) was an attempt to give an atomistic explanation to this phenomenon in terms of the concept of 'virtual bound state' which was first introduced by Friedel (1954) to solid state problems. In brief, the nearest neighbour distance

continuous electronic transition occuring in liquid caesium. In what follows, the numerical calculations of the resistivity based on the virtual bound state model described earlier and employing the highly successful Ziman's theory of liquid metals are described in some detail.

## 4. Resistivity of a two-species System

The resistivity of a monoatomic liquid metal, according to Ziman's theory (Ziman 1964) is given by,

$$\rho = \frac{12\pi\Omega_0}{e^2\hbar v_F^2} \int_0^1 S(x) |V(x)|^2 x^3 \, dx \qquad (2)$$

where V(X) represents the electron-ion form factor and S(X) is the usual structure factor. $X = q/2k_F$ where q is the momentum transfer vector and $k_F$ is the Fermi momentum. Under conditions of virtual bound state formation, the electron-ion form factor becomes complex (this is discussed in detail in the next section) and the resistivity formula takes the form

$$\rho = \frac{12\pi\Omega_0}{e^2\hbar v_F^2} \int_0^1 Z x^3 \, dx \qquad (3)$$

where

$$Z = c S_{BB}(x) V_B(x) V_B^*(x) + (1-c) S_{AA}(x) V_A^2(x) + 2[c(1-c)]^{1/2} S_{AB}(x) V_A(x) \{V_0(x) + V_d'(x)\}$$

Here C represents the concentration of the collapsed species. $S_{AA}(X)$, $S_{BB}(X)$ and $S_{AB}(X)$ represent the partial structure factors of the system corresponding to the A-A, B-B and A-B interaction. $V_B(X)$ is the complex form factor describing the conduction electron-collapsed species interaction. $V_0(X) + V_d'(X)$ is the real part of the form factor. The presence of the weightage factor $X^3$ in the integrand emphasises that the region $X \sim 1$ corresponding to back scattering on the Fermi surface makes a significant contribution to the resistivity.

It is evident from the relation (3) that a calculation of the resistivity of a two-species system requires a knowledge of the partial structure factors, the form factors and the concentration of the collapsed species as a function of pressure. The partial structure factors of a binary system can, in principle, be obtained experimentaly using the anomalous scattering technique (Ramesh and Ramaseshan, 1971). However it is unlikely that these methods can be utilised in the case of liquid caesium, for the X-ray form factors would be nearly the same for the normal and collapsed species. In view of these experimental difficulties, the highly successful Percus-Yerick theory of binary liquid mixtures was utilised to evaluate the partial structure factors at various pressures. It must be mentioned that considerable amount of experimental information such as the isothermal compressibility, high pressure x-ray diffraction data were used to fix up the parameters that

are required to compute the partial structure factors (for details refer to the paper by Ramesh, 1973). A typical set of partial structure factors is given in Figure 4. The evaluation of the form factors is of central importance in this formulation and is considered in detail in the next section.

## 5. Electron-ion Scattering Amplitude

The phenomenon of resonance scattering is well-known (Messiah, 1965). In the present model we hypothise that when a special interatomic distance is favoured in the liquid phase, a conduction electron possessing the 6S character is resonantly scattered to the 5d state. The formation of a virtual bound state as the 5d band approaches the 6S conduction band is equivalent to the d-component of the scattering amplitude passing through resonance. The d-wave scattering amplitude is given by the partial wave formula (Messiah 1965),

$$f_d(E,\theta) = \frac{2l+1}{R} P_l(\cos\theta) \exp[i\delta_l(E)] \sin\delta_l(E) \quad \ldots\ldots(4)$$

Here $\delta_l(E)$ represents the phase shift associated with the lth partial wave and is of prime importance in evaluating the scattering amplitude. The Legendre polynomial $P_l(\cos\theta)$ describes the angular variation of the scattering amplitude. The behaviour of the phase shift $\delta_l(E)$ near the resonance energy level $E_d$ is well described by the formula

$$\tan\delta_l(E) = \Gamma / 2(E_d - E) \quad (5)$$

Here $\Gamma$ represents the half width of the d-wave resonance. Thus the general formula given in relation (4) under conditions of resonance scattering transforms to,

$$f_d(E,\theta) = \frac{2l+1}{R} P_l(\cos\theta) \frac{\Gamma}{2(E_d - E) - i\Gamma} \qquad (6)$$

The scattering amplitude associated with all the other partial waves is represented by $f_0$ and this approximately describes the electron-normal species interaction. Thus the normal species (referred to as A species) and the collapsed B species are characterised by the scattering amplitudes

$$\begin{aligned} f_A &= f_0 \\ f_B &= f_0 + f_d' + i\, f_d'' \end{aligned} \qquad (7)$$

Here $f_d'$ and $f_d''$ are the real and imaginary components of the d-wave scattering amplitude given by the relation (6). The notation is similar to the one used in the anomalous scattering of X-rays. It is clear that the scattering amplitude associated with the collapsed species is essentially complex. The physical significance of the imaginary component of the scattering amplitude is contained in the optical theorem of the scattering theory through the relation

$$\sigma = \frac{4\pi}{R} f_d''(0) \qquad (8)$$

is the scattering cross-section and $f_d''(0)$ is the imaginary

component of the complex scattering amplitude in the exact forward direction. The electron-ion form factor can be obtained from the scattering amplitude using the t-matrix formulation (Ziman, 1969). In this approach, the screened d-wave form factor is given by

$$V_d(E,\theta) = -\frac{2\pi\hbar^2}{m\Omega_0 \epsilon(X)} f_d(E,\theta) \qquad (9)$$

where $\epsilon(X)$ is the Hartree static dielectric function. Thus $V_0$, $V_d'$ and $V_d''$ represent the screened form factors associated with $f_0$, $f_d'$ and $f_d''$ respectively.

It is clear that a calculation of the form factor requires a knowledge of the two parameters $\Gamma$ and $E_d-E$. For $\Gamma$, a value of 0.1 RY, in confirmity with Ham's Band structure calculations (Ham 1962) seems appropriate. For the present discussion we treat $E_d-E$ as an adjustable parameter though in a later section, a more consistent procedure for fixing this parameter is given. Figure 5 shows the variation of $V_d''(X)$ with $X(=\sin\theta/2)$ assuming $E_d-E = \Gamma/2$. For this particular choice, the screened form factors $V_d'$ and $V_d''$ are identical except for a phase difference of $\pi/2$ between them. The sudden dip in $V_d''$ near $X \sim 1$ corresponding to back scattering on the Fermi surface is the main feature of the d-wave resonance. This aspect almost dictates the observed resistivity behaviour (Figure 3). The normal form factor $V_0$ taken from the work of Bortolani and Calandra (1970) is also shown in the Figure 5.

As remarked previously, the central quantity involved in evaluating the d-wave scattering amplitude is $\delta_l(E)$, the phase shift of the l = 2 partial wave. Thus a knowledge of just $\delta_2$ alone, evaluated at the Fermi energy, is sufficient to arrive at the appropriate form factor. Further an estimate of $\delta_2$ can be made using the Friedel Sum rule viz.,

$$Z \simeq \frac{2}{\pi} \sum_l (2l+1)\, \delta_l(E_F) \qquad (10)$$

where Z represents the screening charge around each of the ions in the liquid. While applying this relation to the system of interest, a plausible assumption that $\delta_2$ makes the dominant contribution to the screening charge around the collapsed atom was made (Ramesh, 1973). A value of $\delta_2(E_F) \simeq \pi/10$ estimated using the Friedel Sum rule was also found to be consistent with the at initio calculations of Stocks et al (1972) on the energy dependence of the d-wave phase shift. It must however be noted that the angular variation of the form factor $V_d''(X)$, evaluated using this value of $\delta_2$, remains the same although its magnitude is reduced in the region $X \sim 1$.

## 6. Results and Discussion

The theoretical curves of the resistivity of liquid caesium evaluated as a function of pressure are given in Figure 3. Curve (a) corresponds to the choice $E_d - E = \Gamma/2$ used in evaluating the d-wave phase shift while curve (b) represents the calculations based on the more consistent value of $\delta_2(E_F)$ estimated using Friedel Sum rule.

The resistivity minimum observed in the low pressure region is a general feature of the alkali metals (except Lithium) both in the solid and liquid phases and was first observed by Bridgman (1949). In the solid phase, the initial decrease in resistivity is connected with the change in the lattice vibrational spectrum and is governed by the Bloch-Gruncisen relation. However the behaviour observed in the liquid phase had not been explained. Ramesh (1973) proposed a simple explanation for the observed behaviour which holds good for the other alkali metals as well. In brief, the argument runs as follows. In the low pressure region the concentration of the collapsed species is so small that for all qualitative purposes, one can treat the liquid as a one-component system. The initial decrease in the isothermal compressibility with pressure leads to a reduction in the magnitude of $S_{AA}(0)$, the long wave-length limit of the structure factor in accordance with the Ornstein-Zernicke compressibility formula. Thus the contribution to the resistivity integral from the region of small momentum transfer known as 'plasma resistance' decreases with pressure. On the other hand the increase in $k_F$ with pressure causes the upper limit of integration in the resistivity formula to sample regions of higher values of $S_{AA}(X)$ so that the 'structural resistance' increases with pressure. The numerical calculations showed that the former effect predominates over the latter leading to the observed resistivity minimum at low pressures.

The steep resistivity increase in the 20-40 kbar region is a direct manifestation of the resonance scattering

of the conduction electrons by the collapsed species. Both the curves (a) and (b) generally explain this behaviour. The qualitative discrepancy between curve (b) and the experimental curve has been explained as due to the inherent limitations of the Ziman's resistivity formula rather than that of the model itself (Ramesh, 1973).

## 7. Cerium - The Kondo Element

Cerium, the first member of the rare-earth series, is an archetypal system showing very interesting phenomena such as the pressure induced isostructural $\gamma$-$\alpha$ transition, a mixed valence in the $\alpha$-phase and a solid-solid phase boundary terminating at a critical point (Gschneidner 1977 and references therein, Robinson 1979). All these phenomena basically stem from the presence of a 4f state which is in close proximity with the Fermi level. The relative position of these two levels can be varied either by pressure or temperature. The $\gamma$-phase of Ce, having a well defined magnetic moment, is generally modelled as an 'Anderson lattice' which consists of a periodic array of highly correlated local electronic states (namely the 4f states) which are embedded in and hybridized with the itinerant states of 6S-5d conduction band.

A 'Kondo lattice' is a special case of an Anderson lattice in which there is a local moment on each lattice site with a favourable antiferromagnetic exchange interaction. Typical examples of Kondo lattice or Kondo compounds are $CeAl_2$ and $CeAl_3$ (Coqblin et al, 1976, Bredl et al, 1978),

$\beta$-Ce (Gschneidner, 1977) and $\gamma$-Ce (Ramesh and Shubha, 1980; Shubha and Ramesh, 1981). These Kondo compounds exhibit a 'Kondo-like' logarithmic decrease in the resistivity in a certain temperature regime which is similar to that observed in dilute systems. The most striking behaviour of the dilute systems (where in magnetic impurities are dissolved in a non-magnetic host) is that instead of electrical resistivity becoming independent of temperature at low temperatures (as it would for a non-magnetic alloy) it increases logarithmically with the decrease of temperature. The combination of this anomalous magnetic scattering and the usual phonon contribution to the resistivity, give a minimum in the total resistivity. Kondo (1964, 1965) showed that these anomalies arise from repeated spin scattering between the impurity and the conduction electrons. The conduction electrons have spin 1/2 and can be flipped from $+\frac{1}{2}\hbar$ to $-\frac{1}{2}\hbar$ by the impurity whose spin S takes up this change in the angular momentum. Kondo showed that the scattering rate appropriate to the conduction electron-impurity moment interaction when calculated beyond the first-Born approximation exhibits a divergence at low temperatures. But marked deviations between the dilute and concentrated system are observed at low temperatures. The current experimental and theoretical situation in this field is well documented in several articles (Maple et al, 1977; Doniach, 1977). The general consensus that comes out of these theoretical models is that there exists a characteristic temperature $T_K$ known as the Kondo temperature around which a gradual transition from the

magnetic to the non-magnetic regime takes place.

Gschneidner et al (1976) observed that $\beta$-Ce (DHCP phase) exhibits an anomalous resistivity behaviour as a function of temperature. The magnetic contribution to the resistivity that was obtained by subtracting the phonon contribution from the total resistivity was found to decrease logarithmically with temperature in the region 80-300°K. It was assumed that the phonon contribution to the resistivity in $\beta$-Ce is the same as that of $\alpha$-La whose structure is identical to that of $\beta$-Ce, but devoid of the effects due to the 4f electrons. Liu et al (1976) were able to expalin successfully the resistivity behaviour of $\beta$-Ce over the entire temperature range and, moreover, to fit the well known formula for Kondo scattering viz.,

$$\rho(T) = \rho_0 \left(1 - a \ln T/T_F\right)$$

to the experimental data in the temperature range 80-300°K.

In this article we review the resistivity behaviour of FCC-phase cerium ($\gamma$-Ce) (Ramesh and Shubha, 1980) and the thermoelectric power (TEP) behaviour of $\gamma$-Ce (Shubha and Ramesh, 1981). Kondo-like logarithmic decrease in the magnetic contribution to the resistivity is observed in these studies in the temperature range 300-500°K. TEP studies over the same temperature range shows a characteristic anomaly. High pressure studies upto 7 kbar reveal a reinforcement of this Kondo character. These experimental observations are discussed on the

basis of a model developed for $\gamma$-Ce wherein a 4f virtual bound state resides just below the Fermi energy. The TEP behaviour of $\gamma$-Ce with temperature compared with that of $\beta$-La showed a large change which is similar to the one predicted by Suhl and Wong (1967). These studies give further support to the model that a 4f VBS lies in close proximity to the Fermi level for $\gamma$-Ce.

8. Experimental

The Ce sample used in these studies were cut from an ingot from Leico company having a purity of 99.9%. X-ray pattern of the annealed Ce sample showed that it was in the pure FCC phase ($\gamma$-Ce). The phononic contribution to the resistivity of $\gamma$-Ce can be experimentally estimated by comparing it with the resistivity of La (FCC phase). $\alpha$-La which has got a DHCP structure at ambient pressure undergone a sluggish transformation to the FCC phase around 23 kbar pressure (Bridgmann, 1954). Some later studies (Piermarini and Weir, 1964; McWhan and Bond, 1964) have shown that as the reverse transformation is also necessarily sluggish, it facilitates the metastable retention of the FCC phase ($\beta$-La) at atmospheric pressure. The sample of La (99.9% purity) used in these studies was initially a mixture of both DHCP and FCC phases. The sample was initially pressurised to about 30 kbar and to increase the kinetics of the conversion, it was heated to 400°C and maintained under these conditions for 2-3 hours. This was followed by a rapid temperature decrease and

then depressurisation of the sample. This cycle of operation was repeated a couple of times for total conversion. X-ray studies confirmed that the sample was fully in the FCC phase. It was found that the magnitude of the resistivity of the sample provided a sensitive probe to detect any remnance of the DHCP phase. The resistivity value of the DHCP phase is around 66 $\mu\Omega$-cm while Spedding and co-workers (as quoted in Burgardt et al 1976) give a value of 54.3 $\mu\Omega$-cm for a sample containing 90% $\beta$ (FCC) and 10% $\alpha$ (DHCP). The resistivity value of the sample used in these studies was about 53 $\mu\Omega$-cm confirming its FCC structure.

Resistivity and TEP studies as a function of temperature from 0-200°C at different pressures were carried out using the teflon cell technique (Reshamwala and Ramesh 1974) with silicone fluid as the pressure transmitter in a conventional piston cylinder apparatus. Automatic recording systems (Shubha and Ramesh 1976, 1977) were used in the collection of experimental data.

## 9. Results

Figure 6(a) gives the resistivity against temperature data for cerium and lanthanum at 7.3 kbar pressure. It is clear that the magnetic contribution to the resistivity obtained by subtracting the resistivity of lanthanum from that of cerium decreases with increase of temperature. Here one is making the same assumption as previous workers (Gschneidner et al 1976) that the phonon contribution in $\gamma$-Ce is the same as that in the FCC phase of La.

Figure 6(b) is the plot of $\Delta\rho = \rho_{Ce} - \rho_{La}$ against ln T at various pressures. The striking feature of this plot is that, beside $\Delta\rho$ against in T being linear, the slope increases markedly with pressure. In fact the slope changes from -13.6 $\mu\Omega$-cm at 1.83 kbar pressure to -20 $\mu\Omega$-cm at 7.3 kbar pressure.

Figure 7 is the plot of TEP of $\gamma$-Ce as a function of temperature upto 200°C at different pressures. The notable feature of this plot is that TEP at 7.3 kbar pressure decreases rapidly with temperature and also has a higher magnitude compared to the other two isobars.

Figure 8 presents the isobars of TEP versus temperature for $\beta$-La. In contrast to the behaviour of $\gamma$-Ce, there is not much variation in TEP as a function of temperature. The experimental evidence in these studies indicate that $\gamma$-Ce is also a 'Kondo compound'. It has been assumed in the analysis of the experimental results that the well known Kondo formula for the magnetic contribution to resistivity in the dilute limit

$$\rho_{\text{magnetic}} = CJ^2S(S+1)\left[1 + JN(0)\ \ln\ (T/T_F)\right] \qquad (14)$$

holds even for a concentrated system in the high-temperature region. Here C is the concentration of magnetic impurities (which for a Kondo compound is one per lattice site), S is the total spin due to the 4f shell and N(0) is the density of states at the Fermi energy for conduction electrons of one spin.

J, the exchange integral connected with s-f exchange scattering is usually approximated as $J = J_0 + J_1$ where $J_0$ ($> 0$) is the usual Heisenberg exchange term while $J_1$ ($< 0$) arises from the covalent admixture between the localised 4f state and the conduction electron states. The anomalous resistivity behaviour arises when J is negative, which can happen when the antiferromagnetic exchange integral $J_1$ predominates over the ferromagnetic term $J_0$. In terms of the transformation described by Schrieffer and Wolff (1966), $J_1$ is given by

$$J_1 \simeq \langle V_{sf} \rangle^2 U / E_f (E_f + U)$$

where $E_f$ is the energy of the 4f virtual bound state relative to the Fermi energy and $\langle V_{sf} \rangle^2$ is related to the half width $\Delta$ of the 4f resonance:

$$\Delta = \pi \langle V_{sf} \rangle^2 N(E_F)$$

U is the usual intra-atomic Coulombic repulsion term in the Friedel-Anderson model. It is clear that a large negative value for $J_1$ can result when $E_f$ lies just below the Fermi energy.

The increase in the slope of the $\Delta\rho$ against ln T plot (Figure 6(a)) with pressure can be understood on the basis of the model wherein 4f virtual bound state exists just below the Fermi energy in $\gamma$-Ce. This would lead to a negative J and, further, there would be a resonant increase in its magnitude with pressure due to the 4f level moving towards the Fermi level.

It is clear from equation (11) that the slope of $\rho$ against ln T is directly proportional to $J^3N(0)S(S+1)$. The upward shift of the 4f state relative to the Fermi energy with increase in pressure causes a decrease in the 'spin' or the magnetic moment. This is obvious from the Anderson model for local-moment formation. However, the increase in N(0) with pressure (Bastide et al 1977) and the resonance enhancement of J predominates over the decelerating term mentioned above.

There is considerable controversy regarding the position of the 4f level relative to the Fermi energy in $\gamma$-Ce; this has an important bearing on the several theoretical models developed for explaining the valence transition (Robinson 1979). Johnson (1974) has theorised that the $\gamma-\alpha$ transition is a Mott transition and that the 4f level is far below the Fermi energy (around 1.8 eV). On the other hand all the promotion models (Blandin et al 1965, Alascio et al 1973) require the 4f virtual bound state to be situated close to the Fermi energy (around 0.1 eV). The experimental results reviewed here further support the promotion model.

The TEP anomaly in $\gamma$-Ce as compared with that of $\beta$-La gives supporting evidence for the Kondo model of this substance. The increase in the magnitude of TEP with pressure has been satisfactorily explained on the basis of VBS model (Ramesh et al 1974). The existence of a resonant state overlapping the conduction band and lying just below the Fermi

level has the effect of contributing an extra density of states at the Fermi level as, $n(E_F) = n_0(E_F) + n_1(E_F)$. The first term is the contribution from the 6S-5d band and the second term is due to the 4f VBS below $E_F$. The contribution to the TEP due to this extra density of states factor at $E_F$ which is proportional to $\left[ d \ln n_1(E)/dE \right]_{E_F}$ is given by

$$Q' = \frac{2\pi k_B^2 T}{3|e|} \cdot \frac{1}{n(E_F)} \cdot \frac{\Delta (E_F - E_f)}{\left[ (E_F - E_f)^2 + \Delta^2 \right]^2}$$

where $E_F$ and $\Delta$ are the position and the width of the 4f VBS respectively. It is clear from the expression that $Q'$ is positive for the case where 4f VBS lies below $E_F$. Further, its magnitude gets resonantly enhanced with the decrease in $E_F - E_f$ due to the application of pressure. However this would not explain the anomalous decrease in TEP with temperature. Suhl and Wong (1967) have considered the behaviour of TEP when Kondo scattering is taken into account. The prediction of this model is given in the inset of Figure 7. It appears plausible that the temperature variation of TEP in $\gamma$-Ce (Figure 7) arises mainly from Kondo-like scattering. It was not possible to study the behaviour of TEP down to low temperature as $\gamma$-Ce transforms to the mixed valent $\alpha$-Ce. However it has been observed that the different isobars are a part of a universal curve like the one shown (inset of Figure 7) but with $T_K$ - the Kondo temperature shifted to higher temperatures with increase

in pressure. The present experimental results strongly support the fact that a 4f VBS lies in close proximity to the Fermi level.

Références

Alascio B, Lopez A and Olmedo CFE 1973 J. Phys F; Metal Phys 3 1324

Bastide JP, Loriers C, Massat H and Coqblin B 1977 Rare Earths and Actinides ed WD Corner and BK Tanner (Bristol, London Institute of Physics) p 66

Blandin A, Coqblin B and Friedel J 1965 Physics of Solids at high pressures ed CT Tomizuka and RM Emrick (New York; Academic) p 233

Bredl CD, Steglich F and Schotte KD 1978 . Phys B 29 327

Bridgmann PW 1949 The Physics of High Pressure (London; Bell) p 282

Bridgmann PW 1954 Proc Am Acad Arts Sci 83 3

Bortolani V and Calandra C 1970 Phys Rev B 1 2405

Burgardt P, Gschneidner KA, Koskenmaki DC, Finnemore DF, Moorman JO, Legvord S, Stassis C and Vyrostek TA 1976 Phys Rev B 14 2995

Coqblin B, Bhattacharjee AK, Cornut B, Gonzalez-Jimenez F, Iblesias-Sicardi JR and Jullien R 1976, J. Magn Magn Mat 3 67

Doniach S 1977 Valence Instabilities and Related Narrow Band Phenomena ed RD Parks (New York; Plenum) p 169.

Friedel J 1954 Advan Phys 3 446

Gschneidner KA, Burgardt P, Legvoid S, Moorman JO, Vyrostek TA and Stassis C 1976 J. Phys F Metal Phys 6 149

Gschneidner KA 1977 Valence Instabilities and Related Narrow Band Phenomena ed RD Parks (New York; Plenum) p 89

Hall HT, Merrill L and Barnett JD 1964 Science 146 1297

Ham FS 1962 Phys Rev 128 82

Jayaraman A, Newton RC and McDonough JM 1967 Phys Rev 159 527

Johansson 1974 Phil Mag 30 469

Kennedy GC, Jayaraman A and Newton RC 1962 Phys Rev 126 1363

Kondo J 1964 Progr Theor Phys (Kyoto) 32 37

Kondo J 1965 Progr Theor Phys (Kyoto) 34 372

Liu SH, Burgardt P, Gschneidner KA and Legvoid S 1976 J.Phys F; Metal Phys 6 L55

Maple MB, Delong LI, Fertig WA, Johnston DC, McCallum RW and Sheiton RN 1977 Valence Instabilities and related narrow band phenomena ed RD Parks (New York; Plenum) p17

McWhan DB and Bond WL 1964 Rev Sci Instrum 35 626

McWhan DB and Stevens AL 1969 Solid State Commum 7 301

Messiah A 1965 Quantum Mechanics (New York; Wiley) p 386

Piermarini GJ and Weir CE 1964 Science 144 69

Ramesh TG and Ramaseshan S 1971 J Phys C 4 3029

Ramesh TG and Ramaseshan S 1972 Phys Lett B 39 308

Ramesh TG 1973 Pramana 1 21

Ramesh TG, Reshamwala AS and Ramaseshan S 1974 Pramana 2 171

Ramesh TG and Shubha V 1980 J Phys F 10 1821

Rapapport E 1968 J. Chem Phys 48 1433

Reshamwala AS and Ramesh TG 1974 J. Phys E Sci Instrum 7 133

Robinson JM 1979 Phys Rep 51 1

Schrieffer JR and Wolff PA 1966 Phys Rev 149 491

Shubha V and Ramesh TG 1976 J Phys E ; Sci Instrum 9 435

Shubha V and Ramesh TG 1977 High Temp-High Press 9 461

Shubha V and Ramesh TG 1981 J Phys F Metal Phys 11 191

Sternheimer R 1950 Phys Rev 78 235

Stocks GM, Gaspari GD and Gyorffy BL 1972 J Phys F 2 L123

Suhl H and Wong D 1967 Physics 3 17

Yoshida T and Kamakura S 1973 Paper presented at the Third Int Conf Liquid Metals

Ziman JM 1964 Advan Phys 13 89

Ziman JM 1969 Elements of Advanced quantum theory (London; Cambridge University Press) p 127.

Caption to Figures

Figure 1 : Phase diagram of caesium

Figure 2 : Schematic diagram of the position of the resonant 5d state in relation to the effective potential

Figure 3 : Relative resistivity versus pressure for liquid caesium

Figure 4 : Partial structure factors of a binary system of normal and collapsed atoms of caesium

Figure 5 : Screened form factor $V_0(X)$ for normal species. The resonant form factor $V_d''(X)$ when $E_d - E = \Gamma/2$ a special case wherein $V_d'(X) = V_d''(X)$

Figure 6(a) : Resistivity against tempe ature for cerium and lanthanum at 7.3 kbar pressure

Figure 6(b) : Magnetic contribution to the resistivity against ln T at various pressures

Figure 7 : Isobars of the TEP against temperature in $\gamma$-Ce. Inset gives the theoretical prediction of Suhl and Wong (1967)

Figure 8 : Isobars of the TEP against temperature in $\beta$-La.

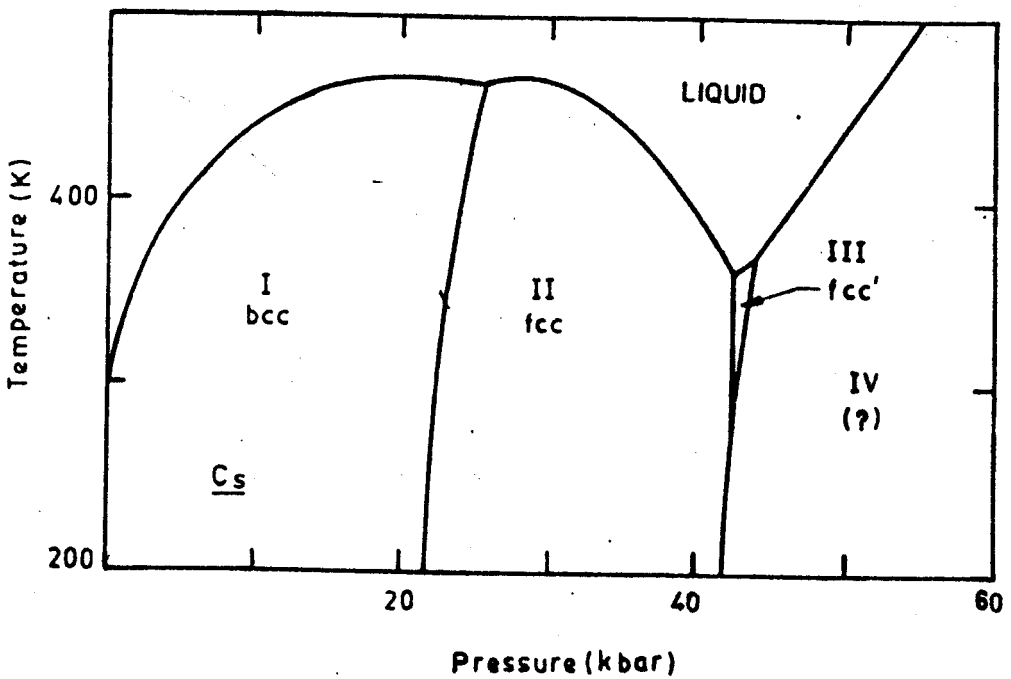
LIQUID
400
200
I
bcc
II
fcc
III
fcc'
IV
(?)
Cs
20
40
60
Temperature (K)
Pressure (kbar)

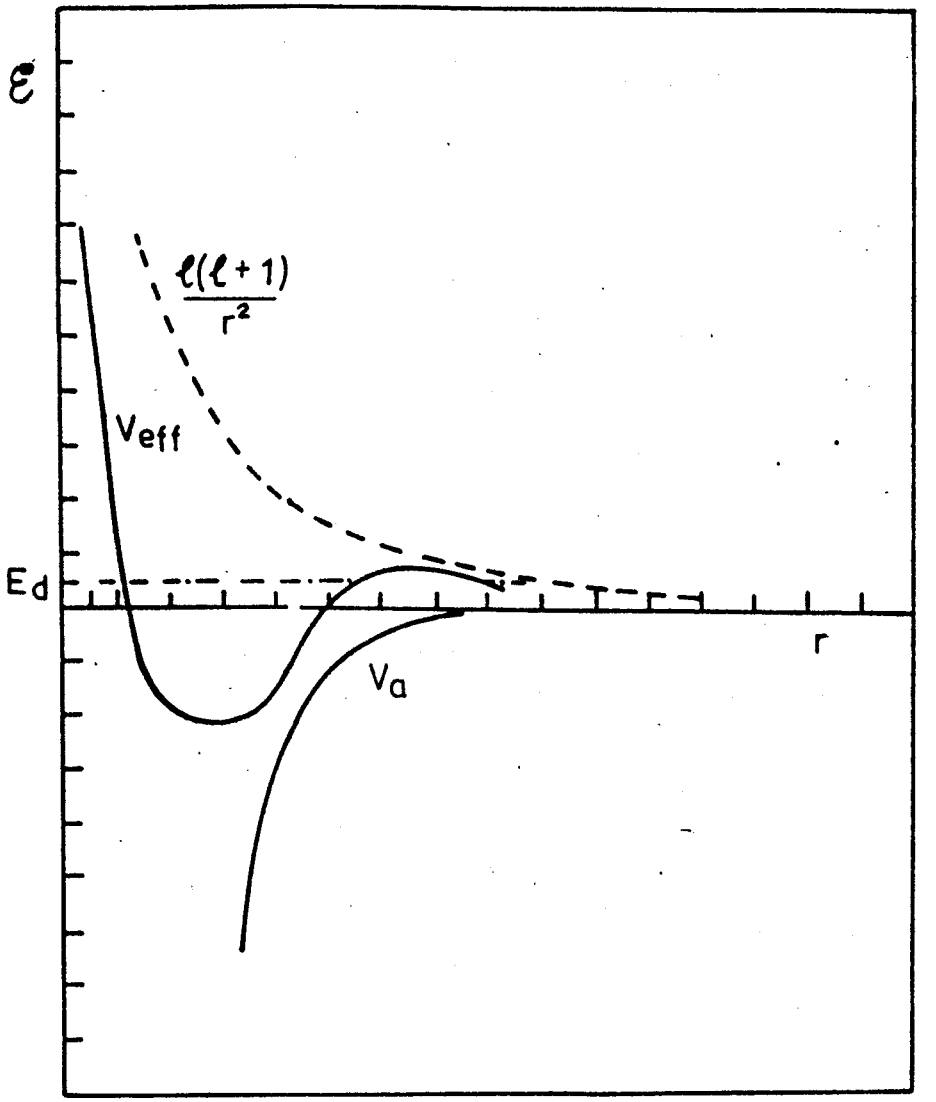
ε
ℓ(ℓ+1)/r²
Veff
Ed
r
Va

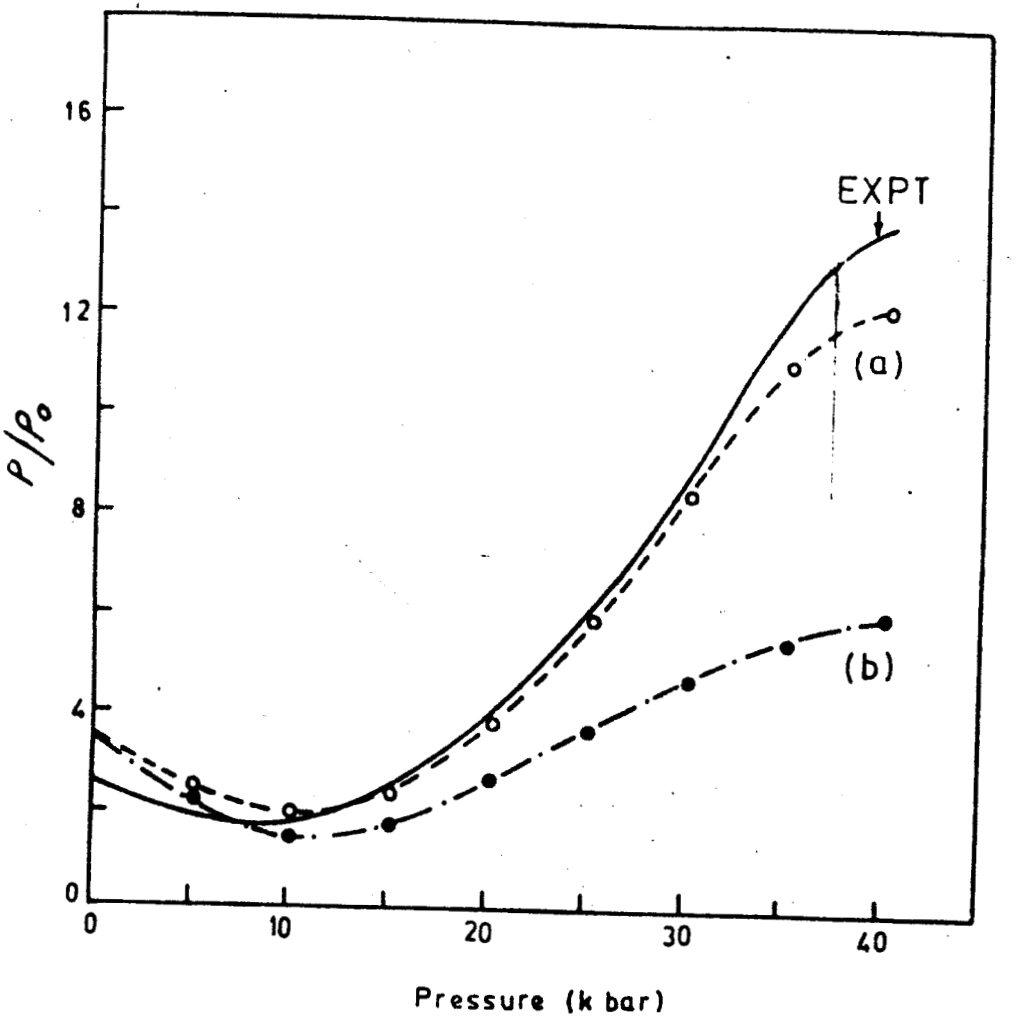
16
12
8
4
0
ρ/ρ₀
EXPT
(a)
(b)
0
10
20
30
40
Pressure (k bar)

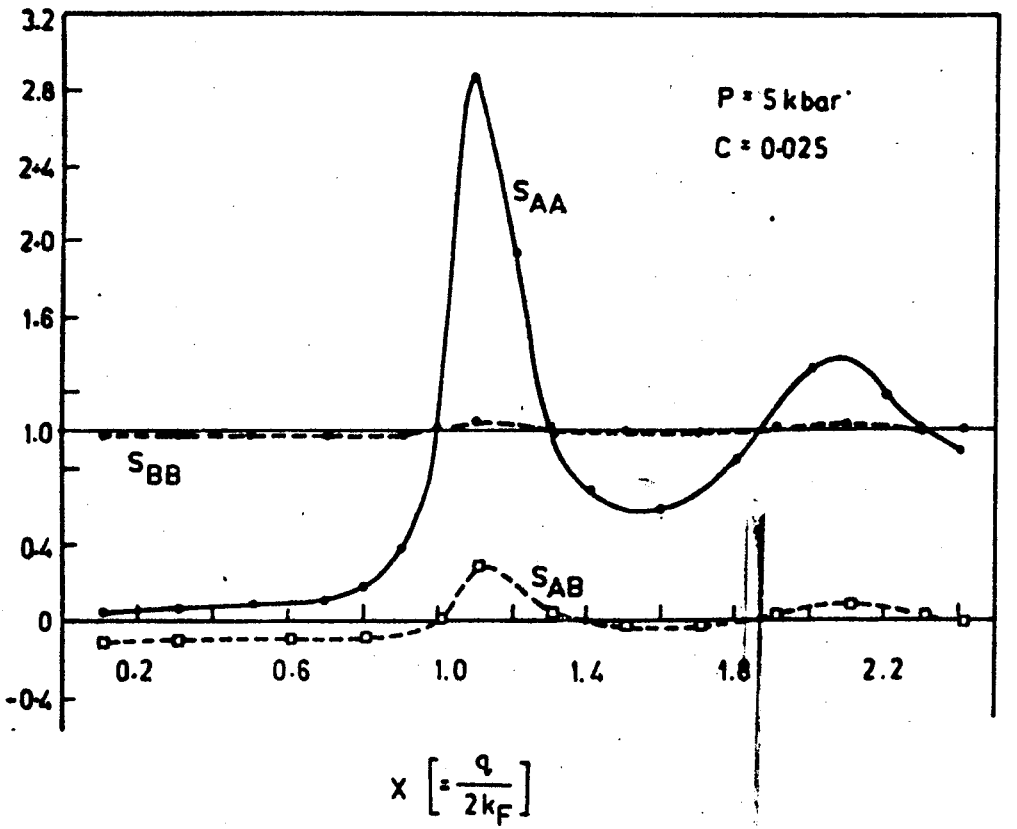
3.2
2.8
2·4
2·0
1.6
1.0
0·4
0
-0·4
0.2
0.6
1.0
1.4
1.8
2.2
P = 5 kbar
C = 0·025
$S_{AA}$
$S_{BB}$
$S_{AB}$
$X \left[ = \frac{q}{2k_F} \right]$

Fig 4

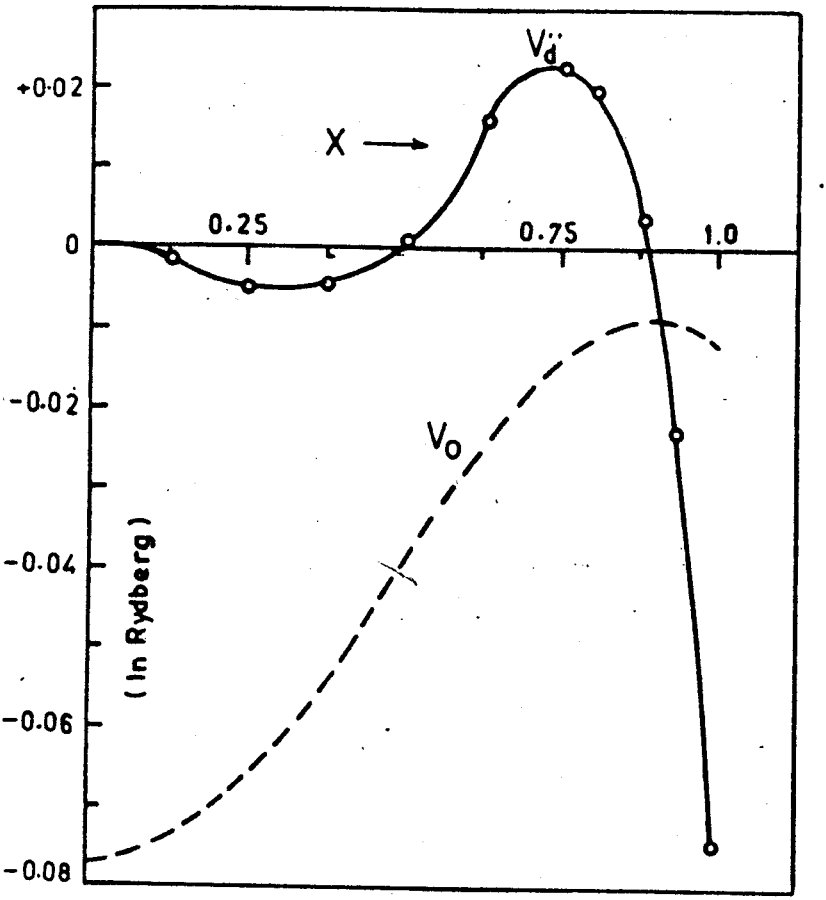
+0·02
0
-0·02
-0·04
-0·06
-0·08
0.25
0.75
1.0
X
$V_d^{ii}$
$V_o$
(In Rydberg)

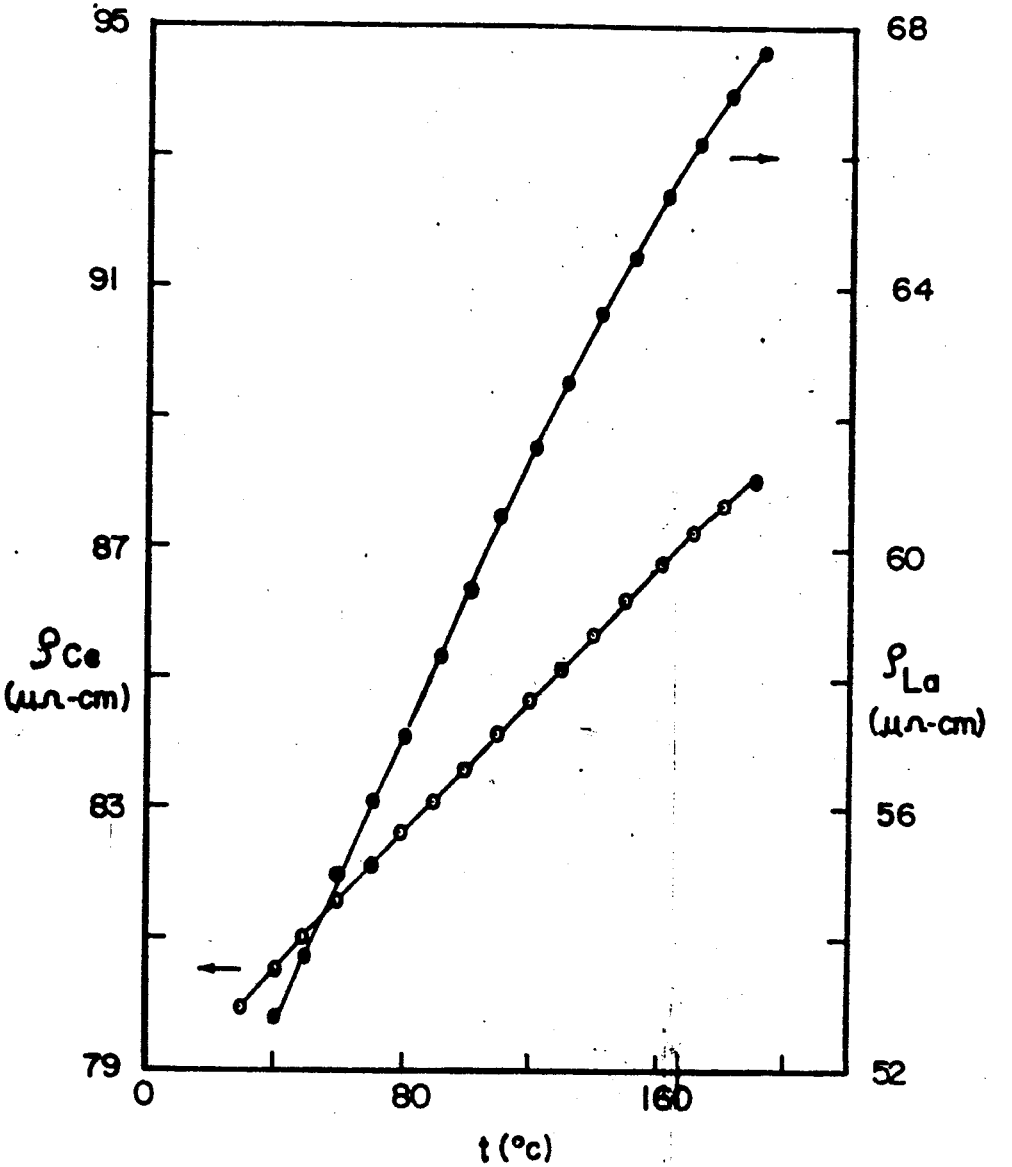
95
91
87
83
79
68
64
60
56
52
0
80
160
t (°c)
ρCe (μΩ-cm)
ρLa (μΩ-cm)

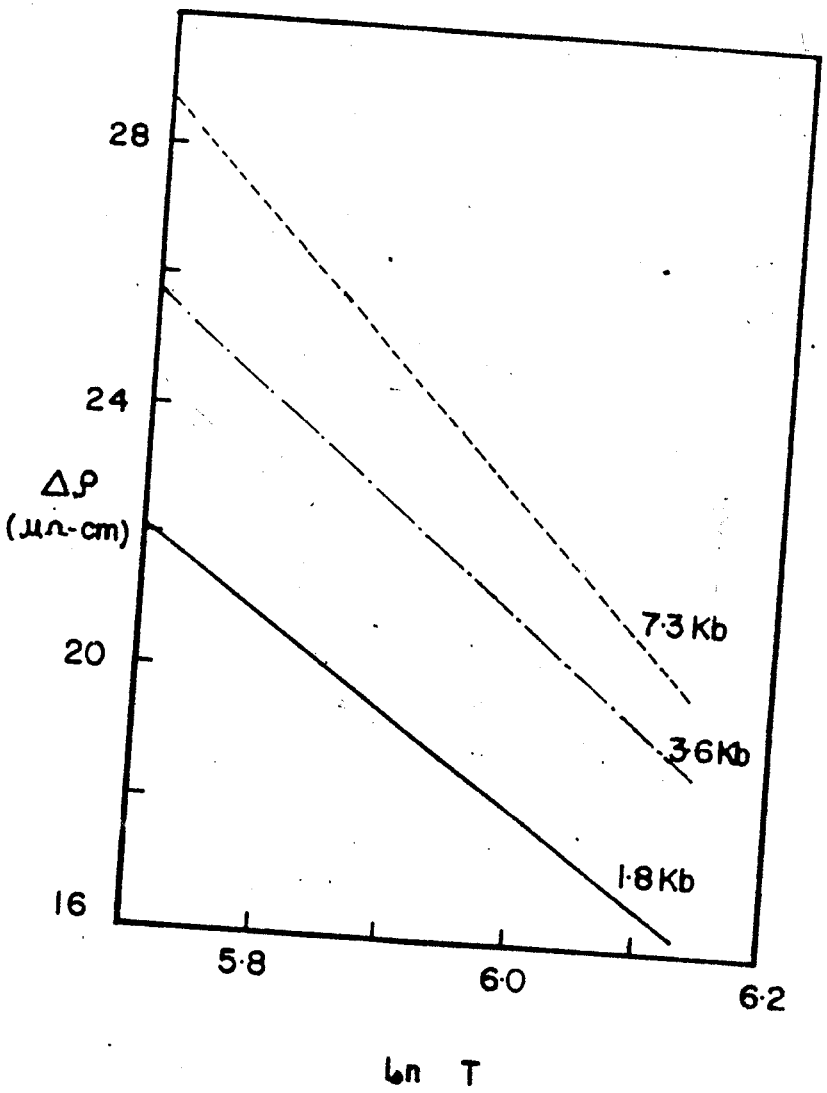
28
24
20
16
Δρ
(μΩ-cm)
7·3 Kb
3·6 Kb
1·8 Kb
5·8
6·0
6·2
ln T

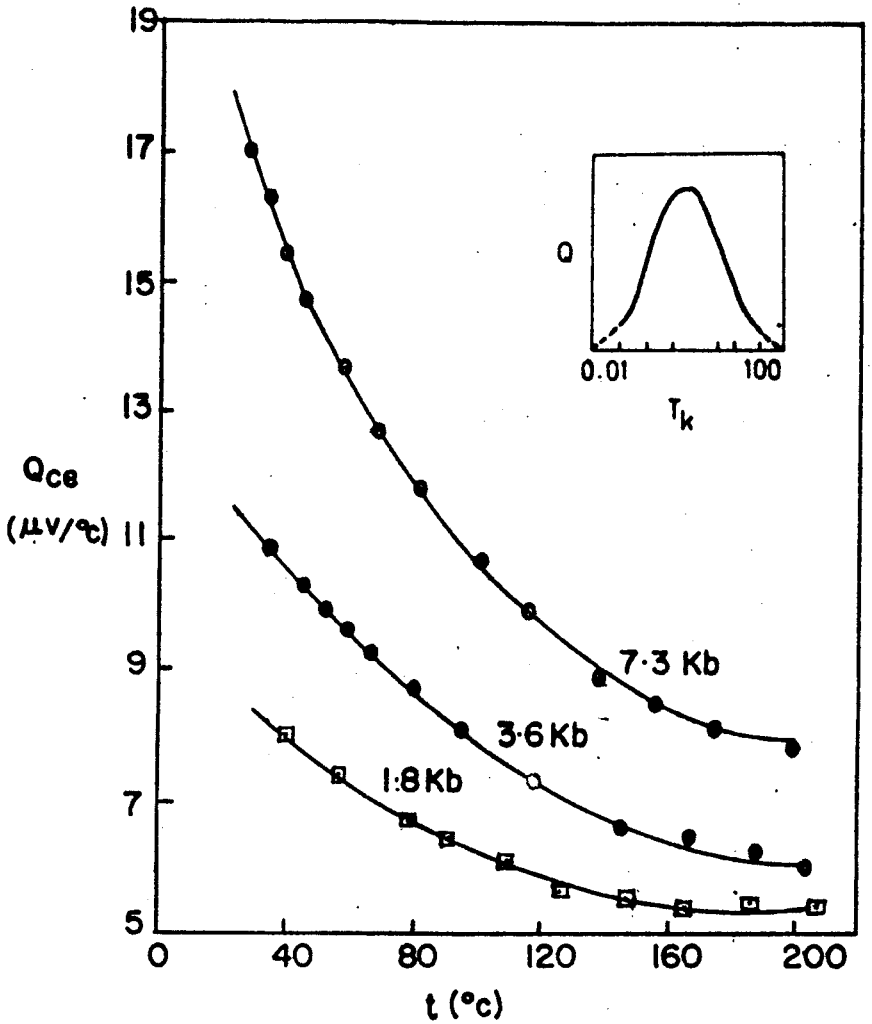
19
17
15
13
11
9
7
5
0
40
80
120
160
200
t (°c)
Qce
(μv/°c)
7·3 Kb
3·6 Kb
1·8 Kb
Q
0.01
100
Tk

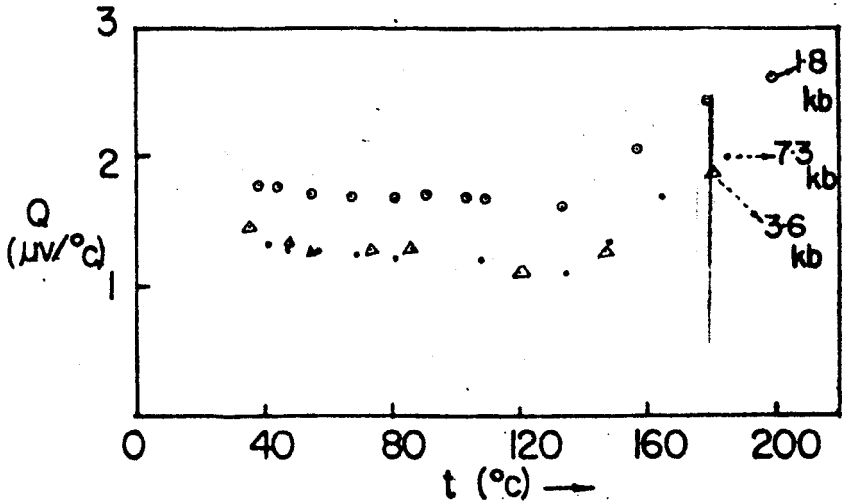
3
2
1
Q
(μV/°C)
0
40
80
120
160
200
t (°C)
1·8
kb
7·3
kb
3·6
kb